Abstract

Purpose: To identify druggable oncogenic fusions in invasive mucinous adenocarcinoma (IMA) of the lung, a malignant type of lung adenocarcinoma in which *KRAS* mutations frequently occur.

Experimental Design: From an IMA cohort of 90 cases, consisting of 56 cases (62%) with *KRAS* mutations and 34 cases without (38%), we conducted whole-transcriptome sequencing of 32 IMAs, including 27 cases without *KRAS* mutations. We used the sequencing data to identify gene fusions, and then performed functional analyses of the fusion gene products.

Results: We identified oncogenic fusions that occurred mutually exclusively with *KRAS* mutations: *CD74-NRG1*, *SLC3A2-NRG1*, *EZR-ERBB4*, *TRIM24-BRAF*, and *KIAA1468-RET*. *NRG1* fusions were present in 17.6% (6/34) of *KRAS*-negative IMAs. The *CD74-NRG1* fusion activated HER2:HER3 signaling, whereas the *EZR-ERBB4* and *TRIM24-BRAF* fusions constitutively activated the ERBB4 and BRAF kinases, respectively. Signaling pathway activation and fusion-induced anchorage-independent growth/tumorigenicity of NIH3T3 cells expressing these fusions were suppressed by tyrosine kinase inhibitors approved for clinical use.

Conclusions: Oncogenic fusions act as driver mutations in IMAs without *KRAS* mutations, and thus represent promising therapeutic targets for the treatment of such IMAs.

Introduction

Oncogene fusions have recently been identified as driver mutations and (possible) therapeutic targets in lung adenocarcinoma (LADC), a major histological type of lung cancer (1). Such fusions include *EML4-* or *KIF5B-ALK, KIF5B* or *CCDC6-RET,* and *CD74-, EZR-,* or *SLC34A2-ROS1* (2-9). These oncogene fusions occur mutually exclusively with one another, and with other targetable oncogene aberrations such as *EGFR, KRAS, BRAF,* and *HER2* mutations. Therefore, molecular targeted therapy combined with the identification of driver oncogene aberrations represents a powerful and promising approach to personalized treatment of LADC (10, 11).

Invasive mucinous adenocarcinoma (IMA) of the lung is composed predominantly of goblet cells. IMA is morphologically characterized by tall columnar cells with basal nuclei and a pale cytoplasm containing varying amounts of mucin (12, 13). IMAs, which constitute 2–10% of all LADCs in Japan, the USA, and European countries (14-16), are indicated as being more malignant than more common types of LADC, such as acinar or papillary adenocarcinoma. The *KRAS* mutation is the only driver aberration commonly detected in IMAs (in 50–80% of cases). To date, no driver gene aberrations have been detected in *KRAS*-negative IMAs; these aberrations must be identified to facilitate the development of effective treatments for such cancers. Therefore, we performed whole-transcriptome sequencing (RNA sequencing) of IMAs lacking *KRAS* mutations to identify novel chimeric fusion transcripts that represent potential targets for cancer therapy.

Materials and Methods

Samples

Ninety IMAs were identified among consecutive patients with primary adenocarcinoma of the lung who were treated surgically at the National Cancer Center Hospital, Tokyo, Japan, from 1998 to 2013. Histological diagnoses were based on the most recent World Health Organization classification and the International Association for the Study of Lung Cancer/American Thoracic Society/European Respiratory Society (IASLC/ATS/ERS) criteria for LADC (13, 17). Total RNA was extracted from grossly dissected, snap-frozen tissue samples using TRIzol (Invitrogen, Carlsbad, CA, USA). The study was approved by the Institutional Review Boards of the participating institutions.

RNA sequencing

RNA sequencing libraries were prepared from 1 or 2 μg of total RNA using the mRNA-Seq Sample Prep Kit or TruSeq RNA Sample Prep Kit (Illumina, San Diego, CA, USA). The resultant libraries were subjected to paired-end sequencing of 50 or 75 bp reads on a Genome Analyzer IIx (GAIIx) or HiSeq 2000 (Illumina). Fusion transcripts were detected using the TopHat-Fusion algorithm (18). Experimental conditions for RNA sequencing are described in **Supplementary Table 1.**

Examinations of oncogenic properties of fusion products.

To construct lentiviral vectors for expression of the CD74-NRG1, EZR-ERBB4 and TRIM24-BRAF fusion proteins, full-length cDNAs were amplified from

tumor cDNA by PCR and inserted into pLenti-6/V5-DEST plasmids (Invitrogen). The integrity of each inserted cDNA was verified by Sanger sequencing. Expression of fusion products of the predicted sizes was confirmed by western blot analysis of transiently transfected and virally infected cells (**Supplementary Fig. 1A**). Details of plasmid transfection, viral infection, western blot analysis, and soft agar colony and tumorigenicity assays are described in **Supplementary Materials and Methods**.

Results and discussion

We prepared an IMA cohort of 90 cases consisting of 56 (62%) cases with *KRAS* mutations and 34 (38%) cases without. The 34 *KRAS*-negative cases included two, one, and one cases with *BRAF* mutation, *EGFR* mutation, and *EML4-ALK* fusion, respectively; the remaining 30 were "pan-negative" for representative driver aberrations in LADCs. Thirty-two cases, consisting of 27 pan-negative and 5 *KRAS* mutation-positive cases, were subjected to RNA sequencing (**Supplementary Table 1**). Analysis of $>2 \times 10^7$ paired-end reads obtained by RNA sequencing and subsequent validation by Sanger sequencing of reverse transcription (RT)-PCR products revealed five novel gene-fusion transcripts detected only in the pan-negative IMAs: *CD74-NRG1*, *SLC3A2-NRG1*, *EZR-ERBB4*, *TRIM24-BRAF*, and *KIAA1468-RET* (**Figs. 1A–B and Table 1;** details in **Supplementary Materials and Methods, Supplementary Fig. 2,** and **Supplementary Table 2**). RT-PCR screening of these fusions in the remaining 58 IMAs that had not been subjected to RNA sequencing revealed one additional pan-negative case with the *CD74-NRG1* fusion. Thus, the *CD74-NRG1* fusion,

detected in 5/34 (14.7%) of cases negative for *KRAS* mutations, was the most frequent fusion among *KRAS* mutation-negative IMAs. Fusions of *CD74* or *SLC3A2* with *NRG1* were present in 17.6% (6/34) of cases. The five novel fusions were mutually exclusively with one another and were not present in any of the *KRAS* mutation-positive cases (**Table 2**).

Four of the novel fusions, *CD74-NRG1*, *SLC3A2-NRG1*, *EZR-ERBB4*, and *TRIM24-BRAF*, involved rearrangements of genes encoding protein kinases or a ligand of a receptor protein kinase (NRG1/neuregulin/heregulin) for which oncogenic rearrangements have not been previously reported in lung cancer (**Supplementary Fig. 3**). The remaining fusion was a novel type involving the *RET* oncogene; fusions with *RET* are observed in 1–2% of LADCs (4, 5, 7, 8, 11). In a screen of 315 LADCs without IMA features from Japanese patients and 144 consecutive LADCs from US patients, all tumors were negative for all of the *NRG1*, *BRAF*, and *ERBB4* fusions, as well as the novel *RET* fusion. Therefore, these fusions might be driver aberrations specific to LADCs with IMA features. The four novel gene fusions were likely to have been caused by inter-chromosomal translocations or paracentric inversion (**Table 1, Supplementary Fig. 3**). Consistently, separation of the signals generated by the probes flanking the translocation sites of *NRG1* in fusion-positive tumors was observed upon fluorescence *in situ* hybridization (FISH) analysis of *CD74-NRG1* fusion positive tumors (**Supplementary Fig. 4**). We also confirmed over-expression of NRG1, ERBB4, and BRAF proteins in tumor cells carrying the corresponding fusions by immunohistochemical analysis, using antibodies recognizing polypeptides retained in the fusion proteins; expression of NRG1,

ERBB4, and BRAF proteins was also observed in some fusion-negative cases (**Supplementary Fig. 5**). IMAs harboring gene fusions were obtained from both male and female patients, although *NRG1* fusion-positive cases were preferentially from female never smokers (**Table 1**).

The CD74-NRG1 and SLC3A2-NRG1 fusion proteins, whose sequences were deduced from RNA sequencing data, contained the CD74 or SLC3A2 transmembrane domain and retained the epidermal growth factor (EGF)-like domain of the NRG1 protein (NRG1 III-β3 form) (**Fig. 1A**). The NRG1 III-β3 protein has a cytosolic N-terminus and a membrane-tethered EGF-like domain, and mediates juxtacrine signals signaling through HER2:HER3 receptors (19). Because parts of CD74 or SLC3A2 replaced the transmembrane domain of wild-type NRG1 III-β3, we speculated that the membrane-tethered EGF-like domain might activate juxtacrine signaling through HER2:HER3 receptors. In addition, it was also possible that expression of these fusion proteins resulted in the production of soluble NRG1 protein due to proteolytic cleavage at sites derived from NRG1 (dashed green lines in **Fig. 1A**), as recently suggested for NRG1 type III proteins (20, 21). Exposing EFM-19 cells to conditioned media from H1299 human lung cancer cells expressing exogenous CD74-NRG1 fusion protein resulted in phosphorylation of endogenous ERBB2/HER2 and ERBB3/HER3 proteins, suggesting that autocrine HER2:HER3 signaling was activated by secreted NRG1 ligands generated from CD74-NRG1 polypeptides (**Fig. 2A**). Phosphorylation of ERK and AKT, downstream mediators of HER2:HER3, was also elevated. HER2, HER3, and ERK phosphorylation was suppressed by lapatinib and afatinib, FDA-approved TKIs that target HER

kinases (22-24). Together, these observations indicate that *NRG1* fusions activated HER2:HER3 signaling by juxtacrine and/or autocrine mechanisms.

The EZR-ERBB4 fusion protein contained the EZR coiled-coil domain, which functions in protein dimerization, and also retained the full ERBB4 kinase domain (**Fig. 1A**). These features indicated that the EZR-ERBB4 protein is likely to form a homodimer via the coiled-coil domain of EZR, causing aberrant activation of the kinase function of ERBB4, similar to the situation of *EZR-ROS1* fusion (5). Indeed, when the *EZR-ERBB4* cDNA was exogenously expressed in NIH3T3 fibroblasts, tyrosine 1258, located in the activation loop of the ERBB4 kinase site, was phosphorylated in the absence of serum stimulation, indicating that fusion with EZR aberrantly activated the ERBB4 kinase (**Fig. 2B**). Consistent with this, phosphorylation of a downstream mediator, ERK, was also elevated. Phosphorylation of ERBB4 and ERK was suppressed by lapatinib and afatinib, which inhibit ERBB4 protein (22-24).

The TRIM24-BRAF fusion protein retained the BRAF kinase domain but lacked the N-terminal RAS-binding domain responsible for negatively regulating BRAF kinase. These features suggested that the fusion was constitutively active, as in the cases of the *ESRP1-BRAF* and *AGTRAP-BRAF* fusions in other cancers (25). When the *TRIM24-BRAF* cDNA was exogenously expressed in NIH3T3 cells, ERK, a downstream mediator of BRAF, was phosphorylated in the absence of serum stimulation, indicating that fusion with TRIM24 aberrantly activated BRAF kinase (**Fig. 2C**). ERK phosphorylation was suppressed by sorafenib, an FDA-approved drug originally identified as a RAF kinase inhibitor (26), and also by the MEK

inhibitor U0126 (**Fig. 2C**).

Exogenous expression of fusion gene cDNAs induced anchorage-independent growth of NIH3T3 fibroblasts, indicating their transforming activities (**Figs. 2D–F**). This growth was suppressed by the kinase inhibitors that suppressed fusion-induced activation of signal transduction, as described above. NIH3T3 cells expressing *EZR-ERBB4* or *TRIM24-BRAF* fusion cDNA formed tumors in nude mice (**Fig. 3**). Therefore, we concluded that these three fusions function as driver mutations in IMA development. We screened 200 commonly used human lung cancer cell lines, but all were negative for these three fusions (data not shown); thus, the oncogenic properties of these fusions remain unvalidated in human cancer cells.

The results here suggest that the *NRG1*, *ERBB4* and *BRAF* fusions are novel driver mutations involved in the development of IMAs of the lungs (**Fig. 1C**) and potential targets for existing TKIs. The recurrent *NRG1* fusions were especially notable because NRG1 was previously identified as a regulator of goblet-cell formation in primary cultures of human bronchial epithelial cells (27); therefore, activation of the NRG1-mediated signaling pathway(s) might play a part in IMA development by contributing to both cell transformation and acquisition of goblet-cell morphology. In addition to a small fraction of known druggable aberrations (an *ALK* fusion and an *EGFR* mutation), more than 10% (11/90; 12.2%) of IMAs harbored other druggable aberrations targeted by existing kinase inhibitors: these aberrations were represented by fusions involving *NRG1*, *ERBB4*, *BRAF*, or *RET*, or *BRAF* mutations (**Table 2,**

Fig. 1C). To facilitate translation of these findings to the cancer clinic, it will be necessary to establish diagnostic methods, particularly using break-apart and fusion FISH methods, capable of detecting these aberrations. Such methods will also help identify additional fusions involving other partner genes and contribute to a greater understanding of the significance of gene fusions in lung carcinogenesis.

Disclosure of Potential Conflicts of Interest

The authors declare no conflicts of interest.

Acknowledgments

We thank Suenori Chiku and Hirohiko Totsuka for the analysis of sequencing data and Dai Suzuki, Kazuko Nagase, Sachiyo Mitani, Sumiko Ohnami, Yoko Odaka, and Misuzu Okuyama for technical assistance.

Grant Support

This work was supported in part by the Advanced Research for Medical Products Mining Program of the National Institute of Biomedical Innovation (NIBIO) and Grants-in-Aid from the Ministry of Health, Labor, and Welfare for the Third-term Comprehensive 10 year Strategy for Cancer Control.

Note: Supplementary information is available on the Clinical Cancer Research website.

References

1. Pao W, Hutchinson KE. Chipping away at the lung cancer genome. Nat Med. 2012;18:349-51.

2. Shaw AT, Engelman JA. ALK in lung cancer: past, present, and future. J Clin Oncol. 2013;31:1105-11.

3. Gautschi O, Zander T, Keller FA, Strobel K, Hirschmann A, Aebi S, et al. A patient with lung adenocarcinoma and RET fusion treated with vandetanib. J Thorac Oncol. 2013;8:e43-4.

4. Drilon A, Wang L, Hasanovic A, Suehara Y, Lipson D, Stephens P, et al. Response to Cabozantinib in Patients with RET Fusion-Positive Lung Adenocarcinomas. Cancer Discov. 2013;3:630-5.

5. Takeuchi K, Soda M, Togashi Y, Suzuki R, Sakata S, Hatano S, et al. RET, ROS1 and ALK fusions in lung cancer. Nat Med. 2012;18:378-81.

6. Mano H. ALKoma: a cancer subtype with a shared target. Cancer Discov. 2012;2:495-502.

7. Lipson D, Capelletti M, Yelensky R, Otto G, Parker A, Jarosz M, et al. Identification of new ALK and RET gene fusions from colorectal and lung cancer biopsies. Nat Med. 2012;18:382-4.

8. Kohno T, Ichikawa H, Totoki Y, Yasuda K, Hiramoto M, Nammo T, et al. KIF5B-RET fusions in lung adenocarcinoma. Nat Med. 2012;18:375-7.

9. Ju YS, Lee WC, Shin JY, Lee S, Bleazard T, Won JK, et al. A transforming KIF5B and RET gene fusion in lung adenocarcinoma revealed from whole-genome and transcriptome sequencing. Genome Res. 2012;22:436-45.

10. Oxnard GR, Binder A, Janne PA. New targetable oncogenes in non-small-cell lung cancer. J Clin Oncol. 2013;31:1097-104.

11. Kohno T, Tsuta K, Tsuchihara K, Nakaoku T, Yoh K, Goto K. RET fusion gene: Translation to personalized lung cancer therapy. Cancer Sci. 2013.

12. Travis WD, Brambilla E, Riely GJ. New pathologic classification of lung cancer: relevance for clinical practice and clinical trials. J Clin Oncol. 2013;31:992-1001.

13. Travis WD, Brambilla E, Noguchi M, Nicholson AG, Geisinger KR, Yatabe Y, et al. International association for the study of lung cancer/american thoracic society/european respiratory society international multidisciplinary classification of lung adenocarcinoma. J Thorac Oncol. 2011;6:244-85.

14. Tsuta K, Kawago M, Inoue E, Yoshida A, Takahashi F, Sakurai H, et al. The utility of the proposed IASLC/ATS/ERS lung adenocarcinoma subtypes for disease prognosis and correlation of driver gene alterations. Lung Cancer. 2013;81:371-6.

15. Warth A, Muley T, Meister M, Stenzinger A, Thomas M, Schirmacher P, et al. The novel histologic International Association for the Study of Lung Cancer/American Thoracic Society/European Respiratory Society classification system of lung adenocarcinoma is a stage-independent predictor of survival. J Clin Oncol. 2012;30:1438-46.

16. Yoshizawa A, Motoi N, Riely GJ, Sima CS, Gerald WL, Kris MG, et al. Impact of proposed IASLC/ATS/ERS classification of lung adenocarcinoma: prognostic subgroups and implications for further revision of staging based on analysis of 514 stage I cases. Mod Pathol. 2011;24:653-64.

17. Travis WD, Brambilla, E., Muller-Hermelink, H.K. and Harris, C.C. , editor. *World Health Organization Classification of Tumors;* Pathology and Genetics, Tumours of Lung, Pleura, Thymus and Heart. Lyon: IARC Press; 2004.

18. Kim D, Salzberg SL. TopHat-Fusion: an algorithm for discovery of novel fusion transcripts. Genome Biol. 2011;12:R72.

19. Falls DL. Neuregulins: functions, forms, and signaling strategies. Exp Cell Res. 2003;284:14-30.

20. Fleck D, van Bebber F, Colombo A, Galante C, Schwenk BM, Rabe L, et al. Dual cleavage of neuregulin 1 type III by BACE1 and ADAM17 liberates its EGF-like domain and allows paracrine signaling. J Neurosci. 2013;33:7856-69.

21. Dislich B, Lichtenthaler SF. The Membrane-Bound Aspartyl Protease BACE1: Molecular and Functional Properties in Alzheimer's Disease and Beyond. Front Physiol. 2012;3:8.

22. Majem M, Pallares C. An update on molecularly targeted therapies in second- and third-line treatment in non-small cell lung cancer: focus on EGFR inhibitors and anti-angiogenic agents. Clin Transl Oncol. 2013;15:343-57.

23. Perez EA, Spano JP. Current and emerging targeted therapies for metastatic breast cancer. Cancer. 2012;118:3014-25.

24. Nelson V, Ziehr J, Agulnik M, Johnson M. Afatinib: emerging next-generation tyrosine kinase inhibitor for NSCLC. Onco Targets Ther. 2013;6:135-43.

25. Palanisamy N, Ateeq B, Kalyana-Sundaram S, Pflueger D, Ramnarayanan K, Shankar S, et al. Rearrangements of the RAF kinase pathway in prostate cancer, gastric cancer and melanoma. Nat Med. 2010;16:793-8.

26. Wilhelm SM, Adnane L, Newell P, Villanueva A, Llovet JM, Lynch M. Preclinical overview of sorafenib, a multikinase inhibitor that targets both Raf and VEGF and PDGF receptor tyrosine kinase signaling. Mol Cancer Ther. 2008;7:3129-40.

27. Kettle R, Simmons J, Schindler F, Jones P, Dicker T, Dubois G, et al. Regulation of neuregulin 1beta1-induced MUC5AC and MUC5B expression in human airway epithelium.

Am J Respir Cell Mol Biol. 2010;42:472-81.

Figure 1. Oncogenic fusions in invasive mucinous lung adenocarcinomas (IMAs). **A,** Schematic representations of the wild-type proteins (top rows of each section) followed by the fusion proteins identified in this study. The breakpoints for each variant are indicated by blue arrows. TM: transmembrane domain. Locations of putative cleavage sites in the NRG1 polypeptide are indicated by dashed green lines. **B,** Detection of gene-fusion transcripts by RT-PCR. RT-PCR products for glyceraldehyde-3-phosphate dehydrogenase (*GAPDH*) are shown below. Six IMAs (T) positive for gene fusions are shown alongside their corresponding non-cancerous lung tissues (N); labels below the gel image indicate sample IDs (see **Table 1**). **C,** Pie chart showing the fraction of IMAs that harbor the indicated driver mutations.

Figure 2. Oncogenic properties of gene-fusion products. **A,** ERBB3 activation by *CD74-NRG1* fusion, demonstrated using the EFM-19 cell system. ERBB3, ERBB2, AKT, and ERK phosphorylation were examined in EFM-19 (reporter) cells treated for 30 min with conditioned media from H1299 cells exogenously expressing *CD74-NRG1* cDNA. Phosphorylation was suppressed by HER-TKIs. **B,** ERBB4 activation by *EZR-ERBB4* fusion. Stably transduced NIH3T3 cells were serum-starved for 24 h and treated for 2 h with DMSO (vehicle control) or TKIs. Phosphorylation of ERBB4 and ERK was suppressed by ERBB4-TKIs. EZR-ERBB4 protein was detected using an antibody recognizing ERBB4 polypeptides retained in the fusion protein. **C,** BRAF activation by *TRIM24-BRAF* fusion. Stably transduced NIH3T3 cells were serum-starved for 24 h and treated for 2 h with DMSO or kinase inhibitors. ERK phosphorylation

(activation) was suppressed by sorafenib, a kinase inhibitor targeting BRAF, as well as by U0126, a MEK inhibitor. TRIM24-BRAF protein was detected using an antibody recognizing BRAF polypeptides retained in the fusion protein. **D–F,** Anchorage-independent growth of NIH3T3 cells expressing *CD74-NRG1* (D), *EZR-ERBB4* (E), or *TRIM24-BRAF* (F) cDNA, and suppression of this growth by kinase inhibitors. Mock-, *CD74-NRG1-*, *EZR-ERBB4-*, and *TRIM24-BRAF*-transduced NIH3T3 cells were seeded in soft agar with DMSO alone or kinase inhibitors. Colonies > 100 μm in diameter were counted after 14 days. Column graphs show mean numbers of colonies ± S.E.M.

Figure 3. Tumorigenicity of NIH3T3 cells expressing *ERZ-ERBB4* or *TRIM24-BRAF* fusion cDNAs. **A,** Tumor growth in nude mice injected with NIH3T3 cells expressing empty vector, *EZR-ERBB4* fusion, or *TRIM24-BRAF* fusion. Cells were resuspended with 50% Matrigel and injected into the right flank of nude mice. Tumor size was measured twice weekly for 5 weeks. Data are shown as means ± S.E.M. **B,** Representative tumors were photographed on day 21. The numbers in parentheses indicate the ratio of the number of mice with tumors to the number of mice receiving cell injection.

Author Manuscript Published OnlineFirst on April 11, 2014; DOI: 10.1158/1078-0432.CCR-14-0107
Author manuscripts have been peer reviewed and accepted for publication but have not yet been edited.

Table 1. Characteristics of invasive mucinous lung adenocarcinomas with novel gene fusions

No.	Sample	Sex	Age	Smoking (packs/year)	Gene fusion	Chromosome aberration	Oncogene mutation*	Pathological stage	TTF1	HNF4A
1	301T	M	55	Ever (47)	*CD74-NRG1*		None	1a	-	+
2	AD12-108T	F	68	Never	*CD74-NRG1*		None	2b	-	+
3	AD09-404T	F	78	Never	*CD74-NRG1*	t(5;8)(q32;p12)	None	1a	-	+
4	AD13-199T	F	47	Never	*CD74-NRG1*		None	1b	-	+
5	AD13-223T	F	53	Never	*CD74-NRG1*		None	1a	-	+
6	AD13-379T	F	66	Never	*SLC3A2-NRG1*	t(8;11)(p12;q13)	None	1b	Not tested	Not tested
7	436T	M	61	Ever (41)	*EZR-ERBB4*	t(2;6)(q25;q34)	None	1b	-	+
8	AD08_127T	F	66	Never	*TRIM24-BRAF*	inv7(q33;q34)	None	1a	+	+
9	AD12-119T	M	62	Current (63)	*KIAA1468-RET*	t(10;18)(q21;q11)	None	1a	+	-

**EGFR*, *KRAS*, *BRAF*, and *HER2* mutations and *ALK*, *RET*, and *ROS1* fusions.

Author Manuscript Published OnlineFirst on April 11, 2014; DOI: 10.1158/1078-0432.CCR-14-0107
Author manuscripts have been peer reviewed and accepted for publication but have not yet been edited.

Table 2. Characteristics of 90 invasive mucinous lung adenocarcinomas

Variable	All	Mutation			Fusion					None (%)
		KRAS	*BRAF*	*EGFR*	*CD74-NRG1 or SLC3A2-NRG1*	*EZR-ERBB4*	*TRIM24-BRAF*	*EML4-ALK*	*KIAA1468-RET*	
Total	90 (100)	56 (62.2)	2 (2.2)	1 (1.1)	6 (6.7)	1 (1.1)	1 (1.1)	1 (1.1)	1 (1.1)	21 (23.3)
Age (mean ± SD; years)	67.2 ± 9.7	68.1 ± 9.7	66.5 ± 3.5	50	61.2 ± 11.5	61	66	64	62	68.1 ± 9.6
Sex										
Male (%)	39 (43.3)	28 (50.0)	0 (0)	0 (0)	1 (16.7)	1 (100)	0 (0)	0 (0)	1 (100)	8 (38.1)
Female (%)	51 (56.7)	28 (50.0)	2 (100)	1 (100)	5 (83.3)	0 (0)	1 (100)	1 (100)	0 (0)	13 (61.9)
Smoking habit										
Never-smoker (%)	51 (56.7)	29 (51.8)	2 (100)	1 (100)	4 (66.7)	0 (0)	1 (100)	1 (100)	0 (0)	13 (61.9)
Ever-smoker (%)	39 (43.3)	27 (48.2)	0 (0)	0 (0)	2 (33.3)	1 (100)	0 (0)	0 (0)	1 (100)	8 (38.1)

A

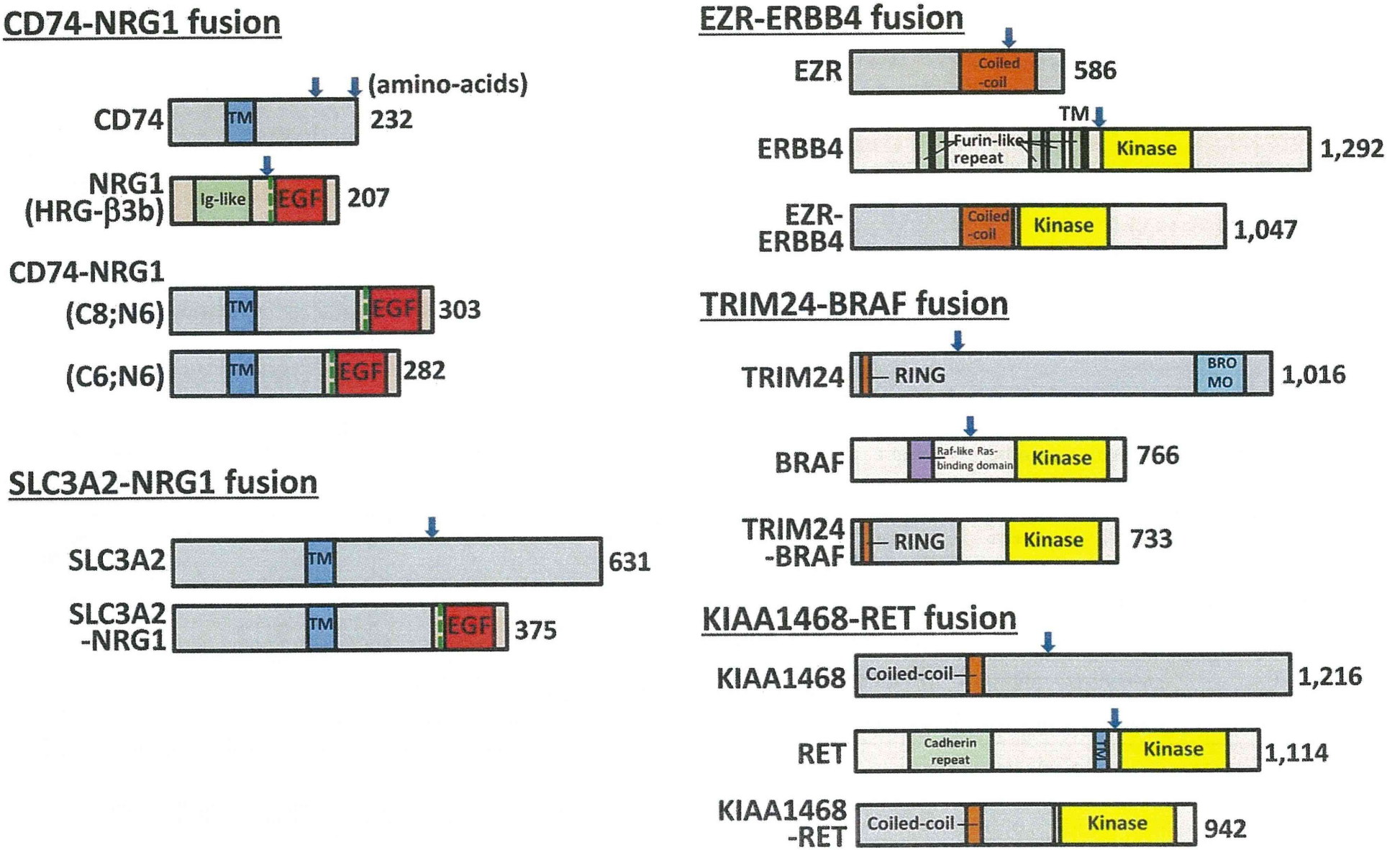

B